**Eastern Kentucky University**
**Encompass**

EKU Faculty and Staff Scholarship

2001

# Data report: Carbon isotopic composition of dissolved CO2, CO2 gas, and methane, Blake-Bahama Ridge and northeast Bermuda Rise, ODP Leg 172

Walter S. Borowski
*Eastern Kentucky University*, w.borowski@eku.edu

Namik Cagatay

Y Tournois

Charles K. Paull
*MBARI*

Follow this and additional works at: https://encompass.eku.edu/fs_research

Part of the Biogeochemistry Commons, and the Geochemistry Commons

# 3. DATA REPORT: CARBON ISOTOPIC COMPOSITION OF DISSOLVED $CO_2$, $CO_2$ GAS, AND METHANE, BLAKE-BAHAMA RIDGE AND NORTHEAST BERMUDA RISE, ODP LEG 172[1]

Walter S. Borowski,[2,3] Namik Cagatay,[4] Yann Ternois,[5] and Charles K. Paull[2,6]

## ABSTRACT

Carbon isotopic data of interstitial dissolved $CO_2$ ($\Sigma CO_2$), $CO_2$ gas, and methane show that a variety of microbial diagenetic processes produce the observed isotopic trends. Anaerobic methane oxidation (AMO) is an important process near the sulfate-methane interface (SMI) that strongly influences the isotopic composition of $\Sigma CO_2$ in the sulfate reduction and upper methanogenic zones, which in turn impacts methane isotopic composition. Dissolved $CO_2$ and methane are maximally depleted in $^{13}C$ near the SMI, where $\delta^{13}C$ values are as light as –31.8‰ and –101‰ PDB for $\Sigma CO_2$ and methane, respectively. $CO_2$ reduction links the $CO_2$ and methane pools in the methanogenic zone so that the carbon isotopic composition of both pools evolves in concert, generally showing increasing enrichments of $^{13}C$ with increasing depth. These isotopic trends mirror those within other methane-rich continental rise sediments worldwide.

## INTRODUCTION

Early diagenetic processes occurring in the pore waters of deep-water, continental-margin sediments are typically mediated by microbial pop-

W.S. Borowski et al.
Carbon Isotopic Composition of CO₂, CO₂ Gas, and Methane

2

ulations. Microbes use various dissolved species to oxidize sedimentary organic matter resulting in modification of the concentration and isotopic composition of dissolved pore-water constituents by removing needed substrates, adding metabolic by-products, and creating a reactive chemical environment (e.g., Richards, 1965; Gieskes, 1981). Carbon transformations particularly reveal these fundamental processes, as organic carbon from sedimentary organic matter is ultimately transformed into $CO_2$ and methane, passing through a cascade of intermediate steps (generally called fermentation reactions).

Terminal carbon transformations of methane-rich diagenetic environments of the world's deep-water continental margins involve several diagenetic processes that are linked by common substrates and/or products. Sulfate reducers utilize interstitial sulfate to oxidize sedimentary organic matter and produce $CO_2$, which dominantly exists in marine pore waters as bicarbonate ($HCO_3^-$). Deeper in the sedimentary section, anaerobic methane oxidation and methanogenesis occur to further affect the concentration and isotopic composition of dissolved $CO_2$ ($\Sigma CO_2$ or dissolved inorganic carbon) and methane.

## Anaerobic Methane Oxidation

At the base of the sulfate reduction zone, microbially mediated anaerobic methane oxidation (AMO),

$$CH_4 + SO_4^{2-} \rightarrow HCO_3^- + HS^- + H_2O,$$

acting near the sulfate-methane interface (SMI), causes both sulfate and methane depletion (Reeburgh, 1976). Deep-water marine sediments on continental margins often show linear sulfate profiles, suggestive of large amounts of sulfate consumption at the SMI caused by AMO (Borowski et al., 1996). Borowski et al. (2000) estimate that at least 35% of interstitial sulfate is consumed by AMO in such settings, highlighting a significant role for AMO in deep-water diagenetic systems.

## Carbon Cycling at the SMI

Carbon cycling is a demonstrably important process at the sulfate-methane interface and within the uppermost methanogenic zone of marine, deep-water continental margins. AMO strongly affects the carbon isotopic composition of the $CO_2$ and methane pools (Borowski et al., 1997) and also induces authigenic formation of carbonate minerals (e.g., Rodriguez et al., 2000). Borowski et al. (1997) showed that AMO, operating over long time spans in an open diagenetic system, induces extreme ^{13}C depletions in both the $CO_2$ and methane pools. For example, at the Blake Ridge, pore water $\Sigma CO_2$ can be as depleted in ^{13}C as –38‰ PDB (Ocean Drilling Program [ODP] Site 995, Borowski et al., 2000), signaling a large contribution of methane carbon to the $CO_2$ pool. Complementary ^{13}C depletions in the methane pool can be as large as –103‰ near the SMI (ODP Site 995, Hoehler et al., 2000). These large ^{13}C depletions near the SMI ripple downward into the underlying sedimentary section. [13]C depletions within $\Sigma CO_2$ and methane occur within the upper methanogenic zone as a consequence of downward diffusion, and because ^{13}C-depleted $\Sigma CO_2$ is used as a substrate in methanogenesis (Claypool and Kaplan, 1974; Borowski et al., 1997; Paull et al., 2000).

## Methanogenesis

Once pore-water sulfate nears depletion in marine sediments, microbially mediated methane production is favored so that dissolved methane concentrations rise in pore waters (Martens and Berner, 1974). Geochemical data from the Blake Ridge, gathered from Deep Sea Drilling Project (DSDP) and ODP drilling, show a connection between the CO$_2$ and methane pools as methanogenesis occurs (e.g., Claypool and Kaplan, 1974; Claypool and Threlkeld, 1983; Galimov and Kvenvolden, 1983). CO$_2$ reduction,

$$CO_2 + 4H_2 \rightarrow CH_4 + H_2O,$$
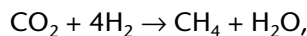
is probably the principal mechanism for biotic methane formation in marine sediments (Whiticar et al., 1986), and the process links these two carbon pools within the methanogenic zone. The isotopic composition of interstitial methane and $\Sigma CO_2$ evolve in concert as $^{12}C$ is preferentially utilized from the $\Sigma CO_2$ pool for methane formation, causing the $\Sigma CO_2$ pool to become depleted in $^{12}C$ (yielding more positive, or heavy, $\delta^{13}C$ values), whereas the methane pool is immediately enriched in $^{12}C$ (yielding very negative, or light, $\delta^{13}C$ values), but progressively accumulates more $^{13}C$ with depth. However with increasing depth, the isotopic composition of $\Sigma CO_2$ and methane begin to diverge with $\Sigma CO_2$ becoming more enriched in $^{12}C$, and methane showing little change in its $\delta^{13}C$ values (e.g., ODP Sites 994, 995, and 997, Borowski et al., 2000; Paull et al., 2000). In other words, the two carbon pools seem to decouple, suggesting a drop in the rate of CO$_2$ reduction, even though sediments are warming along a geothermal gradient (Paull et al., 2000).

## Methane and CO$_2$ Advection

It is likely that a significant proportion of the interstitial methane in the deeper sedimentary section is derived not from in situ production but from methane and/or pore-water transport (Paull et al., 2000). Paull et al. (2000) suggest that upward transport of methane and CO$_2$ affects the carbon isotopic composition of both pools at the Blake Ridge. A model that uses a typical fractionation factor for CO$_2$ reduction ($\Sigma CO_2 \rightarrow CH_4$), that progressively decreases microbial methane production with depth, and that adds methane and CO$_2$ to the lower sedimentary section from deeper below, mimicked typical isotopic profiles seen at the Blake Ridge.

## Blake Ridge

The Blake Ridge region has long been a favored area for geochemical investigations because of its relative geologic simplicity and the presence of gas hydrates (DSDP Leg 11, Sites 102, 103, and 104, Hollister, Ewing, et al., 1972; DSDP Leg 76, Site 533, Sheridan, Gradstein, et al., 1983; and ODP Leg 164, Sites 994, 995, and 997, Paull, Matsumoto, Wallace, et al., 1996) (Fig. F1). ODP Leg 172 continued investigations on the Blake Ridge (Sites 1054–1061) and included sites at the Bahama Ridge (Site 1062) and at the northeast Bermuda Rise (Site 1063) (Keigwin, Rio, Acton, et al., 1998).

Here we report $\Sigma CO_2$ concentrations and the carbon isotopic composition of $\Sigma CO_2$, CO$_2$ gas (derived as a small portion of the $\Sigma CO_2$ pool

**F1.** Map showing DSDP and ODP sites at the Carolina Rise, Blake Ridge, and Bahama Ridge, p. 10.
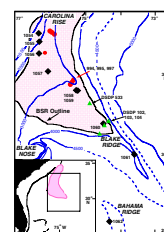
outgasses during sediment recovery), and methane from ODP Leg 172 to add to the global inventory of carbon isotope measurements.

# METHODS

Sediments collected from ODP cores were sampled and processed using standard ODP methods, except that pore waters were sampled more frequently (approximately every 1.5 m) in the upper 50 m of the sedimentary section. Pore waters were extracted from sediments using a hydraulic sediment press (Manheim, 1966) and collected in air-tight syringes (Manheim and Sayles, 1974). At Site 1059, 60-cm$^3$ syringes attached to Reeburgh-style squeezers (Reeburgh, 1967) were used to collect pore waters and interstitial gases from selected samples. This method has the advantage of collecting interstitial gases for isotopic measurements. Sulfate concentration was determined by ion chromatography, and alkalinity was measured by titration (Gieskes et al., 1991). Methane concentrations were measured on board ship using headspace methods and employing a gas chromatograph fitted with a flame ionization detector (FID) (Kvenvolden and McDonald, 1985). Methane concentration measurements gathered using headspace methods were normalized to pore-space volume (e.g., Paull, Matsumoto, Wallace, et al., 1996). Pore-water aliquots for onshore $\Sigma CO_2$ measurements were stored immediately after squeezing in flame-sealed, air-tight ampoules.

Onshore, $\Sigma CO_2$ was separated and purified using cryogenic techniques (e.g., Craig, 1953). Carbon-isotopic-composition measurements of $\Sigma CO_2$ are reported relative to the Peedee belemnite (PDB) standard, and were made using a Delta E mass spectrometer at North Carolina State University. The cumulative (vacuum line and mass spectrometer) accuracy and precision of isotopic measurements are ±0.2‰ and ±0.06‰ (N. Blair, pers. comm., 1998).

Methane and $CO_2$ gases were typically collected directly from core liners using a piercing tool that directed pressured gas into a 60-cm$^3$ syringe (e.g., Paull, Matsumoto, Wallace, et al., 1996). Gas subsamples were taken from syringes, and gas composition and concentration was measured using a gas chromatograph fitted with an FID. Any remaining sample was transferred under water to 60-cm$^3$ serum bottles. In cases where there was insufficient sample to completely fill serum bottles, nitrogen gas was used to fill the bottles leaving only small amounts of water. Thus, contamination with ambient air was avoided. The bottles were sealed with rubber stoppers and metal crimp caps, inverted, and frozen for later measurement in an onshore laboratory.

Gas samples were stripped of their water onshore using cryogenic techniques (e.g., Craig, 1953). $CO_2$ and methane gas fractions were then separated and $\delta^{13}C$ of $CO_2$ gas and methane was measured using a Finnigan MAT 252 gas chromatograph-isotope ratio-mass spectrometer at the University of North Carolina at Chapel Hill following the methods of Merritt and Hayes (1995) and Popp et al. (1995).

Sediment coring during ODP advanced piston coring often results in repeated coring of the same portion of the sedimentary section or lack of sediment recovery over a portion of the sedimentary section within the same hole. Coring of multiple holes at each site allowed a composite stratigraphic section to be constructed that is reported as meters cor-

rected depth (mcd) below the sediment-water interface (see Keigwin, Rio, Acton, et al., 1998).

# RESULTS

Tables T1 and T2 contain concentration and carbon isotopic data for the Carolina Rise (Sites 1054 and 1055), the Blake Ridge (Sites 1058–1061), the Bahama Ridge (Site 1062), and the northeast Bermuda Rise (Site 1063). Figure F2 shows representative concentration-depth profiles of sulfate, alkalinity, and $\Sigma CO_2$, and $\delta^{13}C$ of $\Sigma CO_2$ and methane at Sites 1058 and 1059, which were plotted as a single hole location and are referred to as Site 1058/1059. Figure F3 shows the carbon isotopic composition of $\Sigma CO_2$ and methane, with respect to the SMI, for all sites. Between the sites, the depth of the SMI varies between 10 and 67 mbsf (13 and 75 mcd); the order of increasing depth to SMI at 172 sites is 1058/1059, 1060, 1061, 1055, 1063, 1054, and 1062.

## Dissolved CO$_2$

The carbon isotopic composition of the $\Sigma CO_2$ pool is most depleted in $^{13}C$ at the SMI at all sites, but the intensity of $^{13}C$-depletion varies from site to site (Table T1). Starting at the sediment-water interface, $\Sigma CO_2$ becomes progressively enriched in $^{12}C$ with increasing depth into the sulfate reduction zone, reaching maximum $^{13}C$ depletion ($^{12}C$ enrichment) at the SMI. Site 1058/1059 (–31.8‰ at 8.25 mbsf) exhibits the most depleted $^{13}C$ pool (Figs. F2, F3A), whereas Site 1062 (–20.2‰ at 66.60 mbsf) is least depleted in $^{13}C$ at the SMI (Fig. F3A). The mean value for $\delta^{13}C \Sigma CO_2$ at the SMI is –26.2 ± 5‰; the median value is –28.5‰. Sites in order of increasing $^{13}C$ depletion at the SMI are 1062, 1054, 1055, 1063, 1060, 1061, and 1058/1059.

With increasing depth into the methanogenic zone, $\Sigma CO_2$ generally becomes progressively enriched in $^{13}C$. Maximum $^{13}C$ enrichment occurs at Site 1054 (+12.2‰ at 195.70 mbsf) and minimum $^{13}C$ enrichment occurs at Site 1063 (–2.6‰ at 234.10 mbsf). The mean value of maximum $^{13}C$ enrichment for $\delta^{13}C \Sigma CO_2$ is +4.3 ± 4.8‰; the median value is +3.3‰. The sites in order of increasing $^{13}C$ enrichment are 1063, 1062, 1060, 1061, 1055, 1058/1059, and 1054. The $\delta^{13}C$ values of $\Sigma CO_2$ at Sites 1061 (+3.3‰, 226 mbsf) and 1063 (–2.6‰, 234 mbsf) reach maximum values at ~171 and 215 m into the methanogenic zone, respectively, and then move toward increasing $^{13}C$ depletion with depth.

## Methane

Methane $\delta^{13}C$ values of samples collected from sediment voids range from –65.8 (Site 1054; 197.16 mbsf) to –91.4‰ (Site 1063; 100.66 mbsf) (Table T2; Fig. F3B). The mean and median $\delta^{13}C$ values are –78.1 ± 6.2‰ and –79‰, respectively.

The carbon isotopic composition of methane is most depleted in $^{13}C$ nearest the SMI. Most methane samples are from sediment voids within core liners created by methane degassing during core recovery. Only when methane concentrations reach threshold levels are such gas-filled sediment voids available for sampling. However, at Site 1058/1059, six gas samples were collected in the uppermost methanogenic zone using

T1. Concentration and isotopic data of interstitial constituents from Leg 172 sites, p. 13.

T2. Carbon isotopic composition of interstitial methane and CO$_2$ gas at Leg 172 sites, p. 16.

F2. Pore-water concentration and carbon isotopic composition profiles, p. 11.
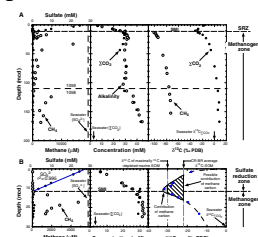
F3. Carbon isotopic values of interstitial dissolved CO$_2$ and methane plotted relative to the SMI, p. 12.
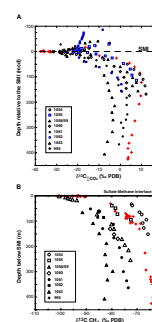
Reeburgh squeezers. The topmost sample has a $\delta^{13}C$ value of –100.6‰, almost 15‰ more depleted than the first sediment void sample at Site 1058/1059, and ~9‰ more depleted than the most negative $\delta^{13}C$ value of any other gas sample from Leg 172.

Methane becomes progressively enriched in $^{13}C$ with increasing depth below the SMI (Fig. **F3B**). Maximum $^{13}C$ enrichment occurs at Site 1054 (–65.8‰, 197 mbsf), whereas $^{13}C$ enrichment (–82.8‰, 416 mbsf) is at a minimum at Site 1063.

# DISCUSSION

Anaerobic methane oxidation is a key process that controls the isotopic composition of $\Sigma CO_2$ and methane near the sulfate-methane interface. Cycling between these two carbon pools within an open system causes large $^{13}C$ depletions (Borowski et al., 1997). Because $\Sigma CO_2$ is so depleted in $^{13}C$ as it enters shallow methanogenic zone, when it serves as the substrate for $CO_2$ reduction the resultant methane is also strongly depleted in $^{13}C$.

$CO_2$ reduction is the dominant methane-forming process within the shallow methanogenic zone of many marine deep-water localities (Whiticar et al., 1986), and the Blake Ridge region is no exception (e.g., Claypool and Kaplan, 1974; Claypool and Threlkeld, 1983; Galimov and Kvenvolden, 1983). Like other methane-rich regions, the carbon isotopic composition of each pool changes concomitantly with depth as $^{12}C$ is preferentially sequestered in methane. However, at some sites (1061 and 1063) the carbon isotopic composition of the pools begins to diverge with increasing depth as the $\Sigma CO_2$ pool becomes progressively enriched with $^{12}C$.

Paull et al. (2000) suggest that lower rates of microbial methane production coupled with delivery of $CO_2$ and methane from below combine to cause this divergence in isotopic trends. Advection perhaps occurs at Leg 172 sites as well, although its effects are usually not observed, probably because of inadequate hole depths. At Sites 1061 and 1063 (the deepest holes), $\delta^{13}C$ $\Sigma CO$ values become slowly but progressively lighter with increasing depth, moving toward typical $\delta^{13}C$ values of Blake Ridge sedimentary organic matter (–21‰; Borowski et al., 1998).

Data from ODP Leg 172 sites at the Blake-Bahama Ridge and Bermuda Rise are consistent with carbon isotopic data for $\Sigma CO_2$ and methane at other Blake Ridge sites (i.e., Sites 533, 994, 995, and 997; see references above) and at other continental margin sites worldwide (Borowski et al., 1997). The processes that create these isotopic trends are pervasive within the world's continental-rise sediments, although many factors combine to control the absolute carbon isotopic composition of $\Sigma CO_2$ and methane.

# CONCLUSION

The dissolved carbon dioxide and methane pools within marine, continental-rise pore waters are geochemically coupled to one another through anaerobic methane oxidation and $CO_2$ reduction. In methane-rich settings, these processes cause consistent trends in isotopic composition that show: (1) maximum depletion of $^{13}C$ of the both pools near

the sulfate-methane interface; and (2) increasing proportions of $^{13}$C in the $\Sigma$CO$_2$ pool with increasing depth in the shallow methanogenic zone. At locations with sufficiently deep holes, $\delta^{13}$C values of $\Sigma$CO$_2$ may become more enriched in $^{12}$C with increasing depth, moving in the direction of the carbon isotopic composition of sedimentary organic matter.

# ACKNOWLEDGMENTS

# REFERENCES

Borowski, W.S., 1998. Pore-water sulfate concentration gradients, isotopic composi-
tions, and diagenetic processes overlying continental margin, methane-rich sedi-
ments associated with gas hydrates. [Ph.D. dissert.]. Univ. of North Carolina,
Chapel Hill, NC.

Borowski, W.S., Hoehler, T.M., Alperin, M.J., Rodriguez, N.M., and Paull, C.K., 2000.
Significance of anaerobic methane oxidation in methane-rich sediments overlying
the Blake Ridge gas hydrates. *In* Paull, C.K., Matsumoto, R., Wallace, P.J., and Dil-
lon, W.P. (Eds.), *Proc. ODP, Sci. Results,* 164: College Station, TX (Ocean Drilling
Program), 87–99.

Borowski, W.S., Paull, C.K., and Ussler, W., III, 1996. Marine pore-water sulfate pro-
files indicate in situ methane flux from underlying gas hydrate. *Geology,* 24:655–
658.

————, 1997. Carbon cycling within the upper methanogenic zone of continental
rise sediments: an example from the methane-rich sediments overlying the Blake
Ridge gas hydrate deposits. *Mar. Chem.,* 57:299–311.

Claypool, G.E., and Kaplan, I.R., 1974. The origin and distribution of methane in
marine sediments. *In* Kaplan, I.R. (Ed.), *Natural Gases in Marine Sediments:* New
York (Plenum), 99–139.

Claypool, G.E., and Threlkeld, C.N., 1983. Anoxic diagenesis and methane genera-
tion in sediments of the Blake Outer Ridge, Deep Sea Drilling Project Site 533, Leg
76. *In* Sheridan, R.E., Gradstein, F.M., et al., *Init. Repts. DSDP,* 76: Washington (U.S.
Govt. Printing Office), 391–402.

Craig, H., 1953. The geochemistry of the stable carbon isotopes. *Geochim. Cosmochim.
Acta,* 3:53–92.

Deines, P., 1980. The isotopic composition of reduced organic carbon. *In* Fritz, P., and
Fontes, J.C. (Eds.), *Handbook of Environmental Isotope Geochemistry* (Vol. 1)*: The Ter-
restrial Environment, A:* Amsterdam (Elsevier), 329–406.

Dillon, W.P., and Paull, C.K., 1983. Marine gas hydrates, II. Geophysical evidence. *In*
Cox, J.L. (Ed.), *Natural Gas Hydrates: Properties, Occurrences, and Recovery:* Woburn,
MA (Butterworth), 73–90.

Galimov, E.M., and Kvenvolden, K.A., 1983. Concentrations of carbon isotopic com-
positions of $CH_4$ and $CO_2$ in gas from sediments of the Blake Outer Ridge, Deep Sea
Drilling Project Leg 76. *In* Sheridan R.E., Gradstein, F.M., et al., *Init. Repts. DSDP,*
76: Washington (U.S. Govt. Printing Office), 403–407.

Gieskes, J.M., 1981. Deep-sea drilling interstitial water studies: implications for chem-
ical alteration of the oceanic crust, layers I and II. *In* Warme, J.E., Douglas, R.G.,
and Winterer, E.L. (Eds.), *The Deep Sea Drilling Project: A Decade of Progress*. Spec.
Publ.—Soc. Econ. Paleontol. Mineral., 32:149–167.

Gieskes, J.M., Gamo, T., and Brumsack, H., 1991. Chemical methods for interstitial
water analysis aboard *JOIDES Resolution. ODP Tech. Note,* 15.

Hoehler, T.M., Borowski, W.S., Alperin, M.J., Rodriguez, N.M., and Paull, C.K., 2000.
Model, stable isotope, and radiotracer characterization of anaerobic methane oxi-
dation in gas hydrate–bearing sediments of the Blake Ridge. *In* Paull, C.K., Matsu-
moto, R., Wallace, P.J., and Dillon, W.P. (Eds.), *Proc. ODP, Sci. Results,* 164: College
Station, TX (Ocean Drilling Program), 79–85.

Hollister, C.D., Ewing, J.I., et al., 1972. *Init. Repts. DSDP,* 11: Washington (U.S. Govt.
Printing Office).

Keigwin, L.D., Rio, D., Acton, G.D., et al., 1998. *Proc. ODP, Init. Repts.,* 172: College
Station, TX (Ocean Drilling Program).

Kvenvolden, K.A., and McDonald, T.J., 1985. Gas hydrates of the Middle America
Trench—Deep Sea Drilling Project Leg 84. *In* von Huene, R., Aubouin, J., et al., *Init.
Repts. DSDP,* 84: Washington (U.S. Govt. Printing Office), 667–682.

Manheim, F.T., 1966. A hydraulic squeezer for obtaining interstitial waters from consolidated and unconsolidated sediments. *Geol. Surv. Prof. Pap. U.S.,* 550-C:256–261.

Manheim, F.T., and Sayles, F.L., 1974. Composition and origin of interstitial waters of marine sediments, based on deep sea drill cores. *In* Goldberg, E.D. (Ed.), *The Sea* (Vol. 5): *Marine Chemistry: The Sedimentary Cycle:* New York (Wiley), 527–568.

Martens, C.S., and Berner, R.A., 1974. Methane production in the interstitial waters of sulfate-depleted marine sediments. *Science,* 185:1167–1169.

Merritt, D.A., and Hayes, J.M., 1995. Carbon isotopic analysis of atmospheric methane by isotope-ratio-monitoring gas chromatography-mass spectrometry. *J.Geophys. Res.,* 100:1317–1326.

Paull, C.K., Lorenson, T.D., Borowski, W.S., Ussler, III, W., Olsen, K., and Rodriguez, N.M., 2000. Isotopic composition of CH$_4$, CO$_2$ species, and sedimentary organic matter within samples from the Blake Ridge: gas source implications. *In* Paull, C.K., Matsumoto, R., Wallace, P.J., and Dillon, W.P. (Eds.), *Proc. ODP, Sci. Results,* 164: College Station, TX (Ocean Drilling Program), 67–78.

Paull, C.K., Matsumoto, R., Wallace, P.J., et al., 1996. *Proc. ODP, Init. Repts.,* 164: College Station, TX (Ocean Drilling Program).

Popp, B.N., Sansone, F., Francis, F.J., and Rust, T.M., 1995. Determination of concentration and carbon isotopic composition of dissolved methane in sediments and nearshore waters. *Anal. Chem.,* 67:405–411.

Reeburgh, W.S., 1967. An improved interstitial water sampler. *Limnol. Oceanogr.,* 12:163–165.

————, 1976. Methane consumption in Cariaco Trench waters and sediments. *Earth Planet. Sci. Lett.,* 28:337–344.

Richards, F.A., 1965. Anoxic basins and fjords. *In* Riley, J.P., and Skirrow, G. (Eds.), *Chemical Oceanography* (Vol. 1): New York (Academic Press), 611–645.

Rodriguez, N.M., Paull, C.K., and Borowski, W.S., 2000. Zonation of authigenic carbonates within gas hydrate–bearing sedimentary sections on the Blake Ridge: offshore southeastern North America. *In* Paull, C.K., Matsumoto, R., Wallace, P.J., and Dillon, W.P. (Eds.), *Proc. ODP, Sci. Results,* 164: College Station, TX (Ocean Drilling Program), 301–312.

Sheridan, R.E., Gradstein, F.M., et al., 1983. *Init. Repts. DSDP,* 76: Washington (U.S. Govt. Printing Office).

Whiticar, M.J., Faber, E., and Schoell, M., 1986. Biogenic methane formation in marine and freshwater environments: CO$_2$ reduction vs. acetate fermentation—isotope evidence. *Geochim. Cosmochim. Acta,* 50:693–709.

**Figure F1.** Map showing the location of DSDP and ODP sites at the Carolina Rise, Blake Ridge, and Bahama Ridge. DSDP Leg 11 Sites 102, 103, and 104 (Hollister, Ewing, et al., 1972) and DSDP Leg 76 Site 533 (Sheridan, Gradstein, et al., 1983) are shown with triangles. ODP Leg 164 sites are shown with circles; Sites 994, 995, and 997 (Paull, Matsumoto, Wallace, et al., 1996) have relevance to this study. ODP Leg 172 sites, noted by diamonds, include those on the Carolina Rise (1054–1057), on the Blake Ridge (1058–1061), and on the Bahama Ridge (1062) (Keigwin, Rio, Acton, et al., 1998). Site 1063 is not plotted on the map but is located ~850 nmi east-northeast of the Blake Ridge on the northeast Bermuda Rise. The stippled areas encompass the region where bottom-simulating reflectors (BSRs) occur, indicative of the presence of gas hydrates within the sediments (Dillon and Paull, 1983).
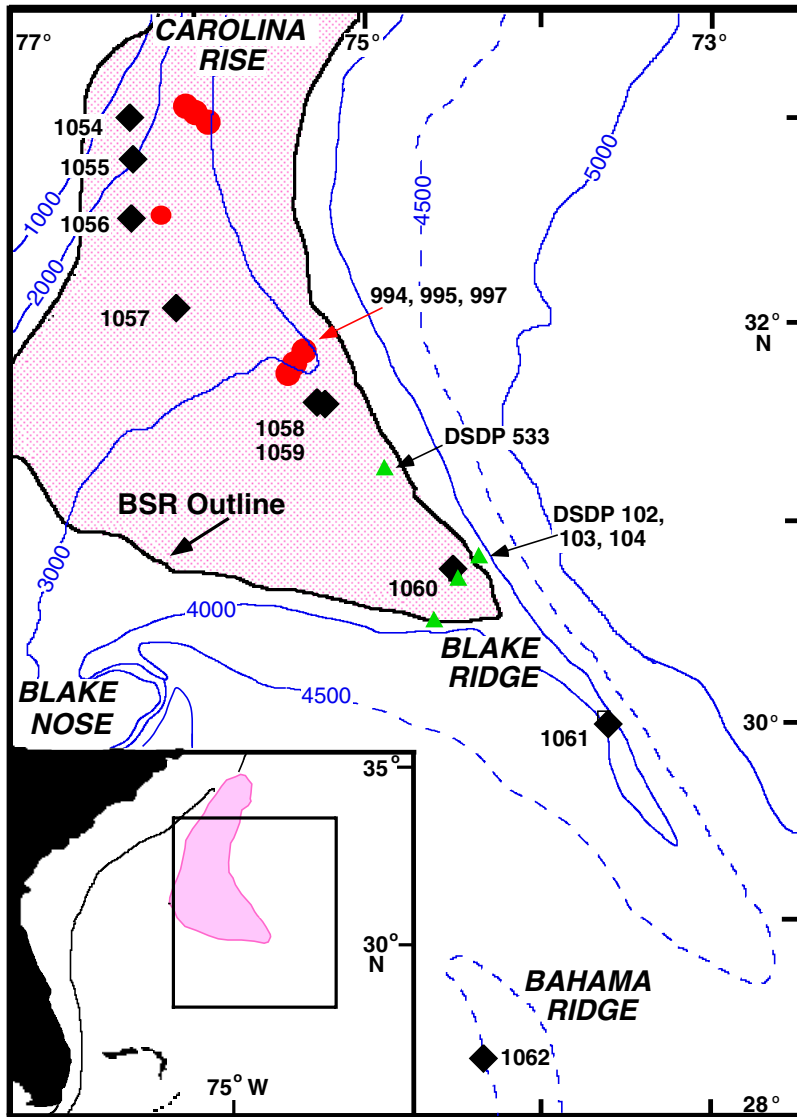
**Figure F2.** Pore water concentration and carbon isotopic composition profiles at Leg 172 Sites 1058 and 1059, plotted as a single hole location (separated laterally by ~4 nmi). Depth is plotted as meters corrected depth (mcd) below the sediment-water interface (see Keigwin, Rio, Acton, et al., 1998, for explanation). Data above 114.31 mcd (96.15 mbsf) are from Site 1059; data below this depth are from Site 1058. **A.** The entire sampled sediment column including the sulfate reduction zone (SRZ) and methanogenic zone. **B.** The upper 30 m of the sediment column showing profiles near the methane-sulfate interface (SMI). Sulfate, methane, $\Sigma CO_2$, and alkalinity values are reported in Table **T1.** Methane concentration is reported as micromolar units (µM)(Keigwin, Rio, Acton, et al., 1998); other concentration units are millimolar (mM). Carbon isotopic values are reported in per mil units (‰, relative to the Peedee belemnite [PDB] standard). $\Sigma CO_2$ isotopic values are tabulated in Table **T1;** methane isotopic values appear in Table **T2.** In the shallow $\delta^{13}C_{\Sigma CO2}$ profile, the shaded portion of the profile illustrates methane carbon in the $CO_2$ pool likely derived from methane through anaerobic methane oxidation, because marine sedimentary organic matter (SOM) is typically more $^{13}C$-enriched than –30‰ PDB (Deines, 1980). The hatched portion of the curve shows carbon likely derived from methane because the isotopic composition of average SOM in sediments of the Carolina Rise and Blake Ridge is –21‰ (e.g., Borowski, 1998). The lower boundary of the curve is defined by a data point (–8.4‰, 33.45 mcd) that is not shown.
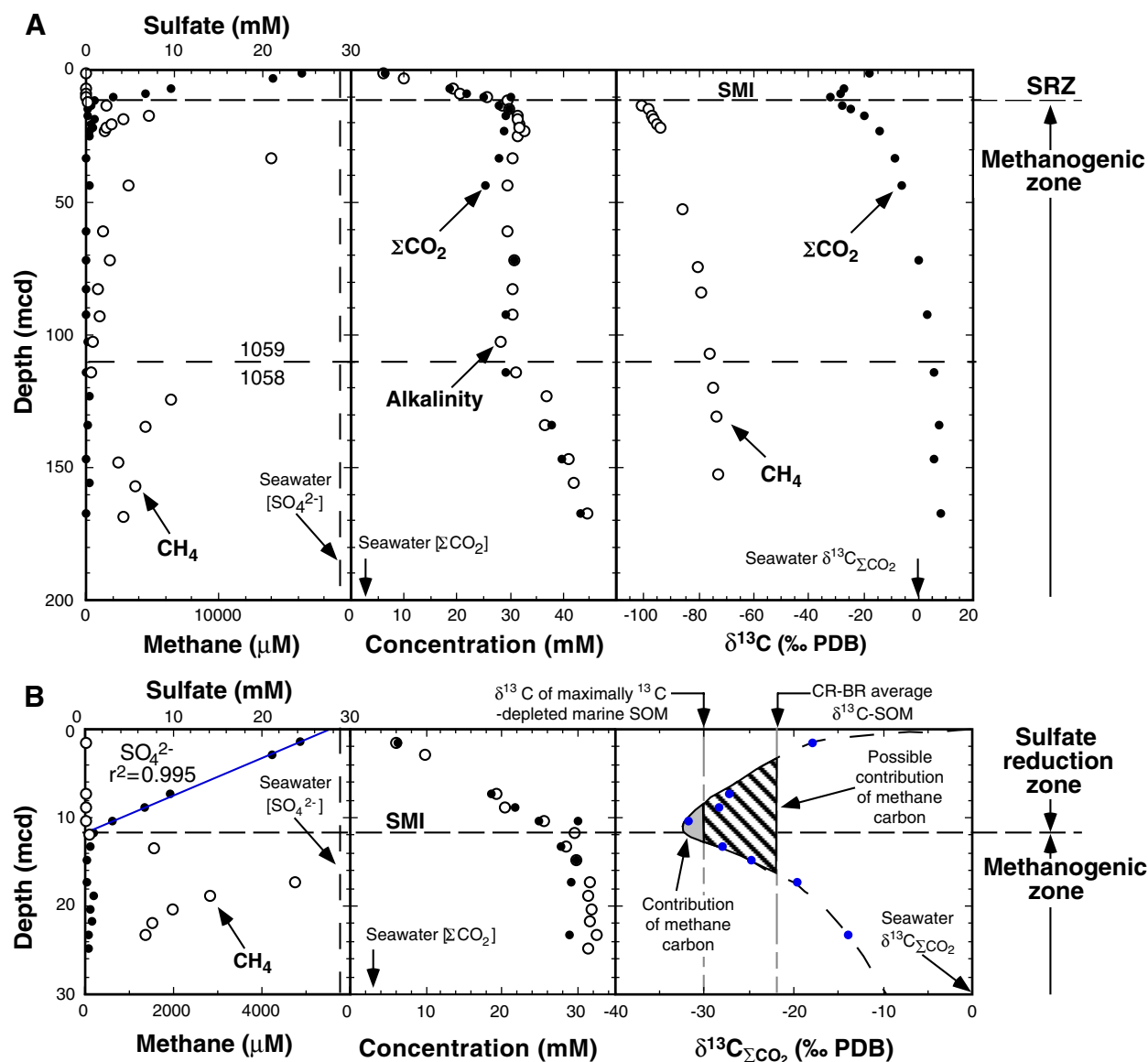
**Figure F3.** (A) Carbon isotopic values of interstitial dissolved CO$_2$ and (B) methane plotted as a function below the seabed in meters (meters corrected depth, mcd; see Keigwin, Rio, Acton, et al., 1998) relative to the sulfate-methane interface (SMI). $\Sigma$CO$_2$ isotopic values are tabulated in Table **T1;** methane isotopic values appear in Table **T2.** Site 995 data (ODP Leg 164) for $\Sigma$CO$_2$ and methane are from Borowski et al. (2000) and Paull et al. (2000), respectively.

**Table T1.** Concentration and isotopic data of selected interstitial constituents from Leg 172 sites. (**See table notes.** Continued on next two pages.)

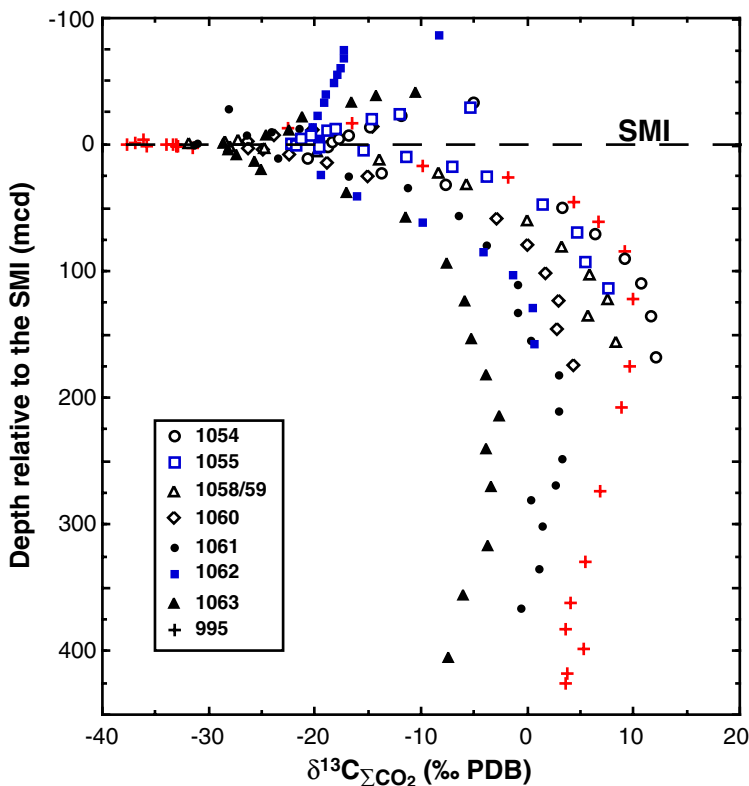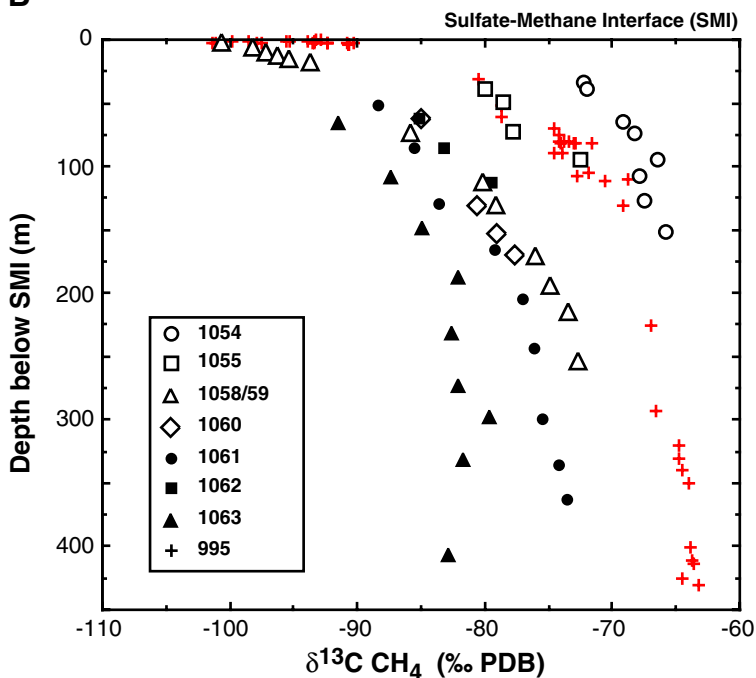| Core, section, interval (cm) | Depth (mbsf) | Depth (mcd) | Sulfate (mM)* | Alkalinity (mM)* | $\Sigma CO_2$ (mM) | $\delta^{13}C\ \Sigma CO_2$ (‰ PDB) |
|---|---|---|---|---|---|---|
| 172-1054A- | | | | | | |
| 1H-1, 145-150 | 1.45 | 1.45 | 27.6 | 4.6 | 4.8 | –5.101 |
| 1H-5, 145-150 | 7.45 | 7.45 | 27.4 | 4.3 | — | — |
| 2H-3, 145-150 | 12.45 | 12.10 | 24.2 | 8.0 | 8.2 | –11.844 |
| 3H-1, 145-150 | 18.95 | 20.20 | 21.0 | 10.9 | 11.4 | –14.732 |
| 3H-6, 145-150 | 26.45 | 27.70 | 16.9 | 16.2 | 14.6 | –16.794 |
| 4H-1, 145-150 | 28.45 | 29.35 | 13.0 | 19.4 | 16.6 | –17.656 |
| 4H-3, 145-150 | 31.45 | 32.35 | 12.1 | 21.8 | 19.2 | –18.338 |
| 4H-6, 145-150 | 35.95 | 36.85 | 10.3 | 23.8 | 20.2 | –18.742 |
| 5H-5, 145-150 | 43.95 | 45.70 | 3.4 | 28.7 | 26.0 | –20.711 |
| 6H-4, 140-150 | 54.90 | 56.75 | 0.0 | 33.5 | 31.9 | –13.71 |
| 8H-1, 140-150 | 63.80 | 66.40 | 0.1 | 37.7 | 34.9 | –7.683 |
| 10H-5, 140-150 | 82.70 | 84.45 | 0.2 | 43.1 | 46.7 | 3.3 |
| 12X-4, 140-150 | 99.40 | 105.49 | 0.1 | 50.7 | 57.1 | 6.4 |
| 14X-4, 140-150 | 118.60 | 124.59 | 0.0 | 55.8 | 62.1 | 9.2 |
| 16X-2, 135-150 | 137.75 | 143.74 | 0.6 | 56.9 | 63.4 | 10.7 |
| 19X-2, 140-150 | 163.80 | 169.79 | 0.5 | 65.2 | 65.0 | 11.6 |
| 22X-4, 140-150 | 195.70 | 201.69 | 0.2 | 67.8 | 67.6 | 12.2 |
| 172-1055B- | | | | | | |
| 1H-1, 145-150 | 1.45 | 1.60 | 27.4 | 3.9 | 4.4 | –5.437 |
| 2H-1, 145-150 | 5.95 | 5.90 | 25.3 | 6.6 | 7.0 | –11.991 |
| 2H-4, 145-150 | 10.45 | 10.40 | 21.1 | 9.0 | 9.2 | –14.593 |
| 3H-1, 145-150 | 15.45 | 18.58 | 11.9 | 13.9 | 13.7 | –18.036 |
| 3H-2, 145-150 | 16.95 | 20.08 | 9.9 | 16.4 | 14.8 | –18.742 |
| 3H-4, 145-150 | 19.95 | 23.08 | 7.1 | 17.9 | 16.4 | –20.401 |
| 3H-6, 145-150 | 22.95 | 26.08 | 4.0 | 19.6 | 17.6 | –21.359 |
| 4H-1, 145-150 | 24.95 | 29.38 | 0.5 | 21.8 | 19.3 | –22.287 |
| 4H-2, 145-150 | 26.45 | 30.88 | 0.3 | 21.0 | 18.3 | –21.73 |
| 4H-3, 145-150 | 27.95 | 32.38 | 0.1 | 21.2 | 19.5 | –19.592 |
| 4H-5, 145-150 | 30.95 | 35.38 | 0.0 | 20.4 | 18.4 | –15.396 |
| 5H-1, 145-150 | 34.40 | 40.12 | 0.1 | 21.2 | 20.3 | –11.445 |
| 5H-6, 140-150 | 41.90 | 47.62 | 0.1 | 23.1 | 21.5 | –7.115 |
| 6H-5, 140-150 | 49.90 | 56.32 | 0.4 | 24.8 | 23.4 | –3.834 |
| 8H-6, 140-150 | 70.40 | 78.21 | 0.1 | 31.6 | 30.7 | 1.4 |
| 10H-6, 140-150 | 89.40 | 99.86 | 0.6 | 38.7 | 34.7 | 4.7 |
| 12H-6, 140-150 | 108.13 | 122.62 | 0.4 | 41.0 | 43.2 | 5.5 |
| 14H-6, 135-150 | 126.43 | 144.16 | 0.2 | 48.5 | 48.4 | 7.7 |
| 172-1058A- | | | | | | |
| 2H-5, 140-150 | 16.90 | 19.35 | 0.2 | 28.2 | 29.1 | — |
| 13H-5, 140-150 | 120.65 | 134.02 | 0.2 | 36.4 | 37.7 | 7.6 |
| 14H-7, 140-150 | 132.80 | 146.79 | 0.0 | 40.9 | 39.7 | 5.8 |
| 16H-5, 140-150 | 148.66 | 167.14 | 0.0 | 44.6 | 43.4 | 8.3 |
| 172-1059A- | | | | | | |
| 1H-1, 145-150 | 1.45 | 1.45 | 24.5 | 6.1 | 6.4 | –17.828 |
| 2H-1, 145-150 | 5.25 | 7.32 | 9.6 | 19.4 | 18.5 | –27.204 |
| 2H-2, 145-150 | 6.75 | 8.82 | 6.7 | 20.5 | 21.7 | –28.361 |
| 2H-3, 145-150 | 8.25 | 10.32 | 3.2 | 25.6 | 25.0 | –31.806 |
| 2H-5, 145-150 | 11.25 | 13.32 | 0.5 | 28.6 | 27.8 | –27.954 |
| 2H-6, 145-150 | 12.75 | 14.82 | 0.2 | 29.8 | 29.8 | –24.668 |
| 3H-1, 145-150 | 14.75 | 17.30 | 0.2 | 31.5 | 29.2 | –19.712 |
| 3H-5, 145-150 | 20.75 | 23.30 | 0.5 | 32.5 | 29.0 | –13.871 |
| 4H-6, 62-72 | 30.42 | 33.45 | 0.0 | 30.6 | 27.8 | –8.36 |
| 5H-5, 150-160 | 39.80 | 43.36 | 0.5 | 29.6 | 25.5 | –5.727 |
| 7H-6, 140-150 | 60.20 | 71.84 | 0.0 | 30.7 | 30.8 | 0.0 |
| 9H-5, 140-150 | 77.70 | 92.56 | 0.0 | 30.6 | 29.3 | 3.2 |
| 11H-5, 140-150 | 96.15 | 114.31 | 0.1 | 31.2 | 29.1 | 5.9 |
| 172-1060A- | | | | | | |
| 1H-1, 145-150 | 1.45 | 1.45 | 25.3 | 6.2 | 5.4 | –16.097 |
| 1H-3, 145-150 | 4.45 | 4.45 | 18.6 | 12.8 | 9.7 | –21.776 |
| 1H-5, 145-150 | 7.45 | 7.45 | 12.2 | 17.5 | 16.1 | –25.28 |
| 2H-1, 145-150 | 10.45 | 12.39 | 3.5 | — | 22.3 | –27.824 |
| 2H-2, 145-150 | 11.95 | 13.89 | 1.3 | 26.9 | — | — |
| 2H-3, 145-150 | 13.45 | 15.39 | 0.8 | 28.2 | — | — |
| 2H-4, 145-150 | 14.95 | 16.89 | 0.2 | 26.2 | 29.1 | –28.926 |
| 2H-5, 145-150 | 16.45 | 18.39 | 0.1 | 25.6 | 27.6 | –27.818 |

## Table T1 (continued).

| Core, section, interval (cm) | Depth (mbsf) | Depth (mcd) | Sulfate (mM)* | Alkalinity (mM)* | ΣCO$_2$ (mM) | δ$^{13}$C ΣCO$_2$ (‰ PDB) |
|---|---|---|---|---|---|---|
| 2H-6, 145-150 | 17.95 | 19.89 | 0.7 | 28.6 | 27.2 | –26.368 |
| 3H-1, 140-150 | 19.90 | 23.90 | 0.1 | 28.6 | 26.7 | –23.961 |
| 3H-5, 140-150 | 25.90 | 29.90 | 0.1 | 27.2 | — | –20.355 |
| 4H-5, 146-156 | 35.46 | 40.08 | 0.2 | 23.6 | 23.5 | –16.421 |
| 5H-5, 144-154 | 44.94 | 50.81 | — | — | 22.7 | –10.633 |
| 7H-5, 140-150 | 63.90 | 74.29 | 0.0 | 24.3 | 21.2 | –4.382 |
| 9H-5, 140-150 | 82.90 | 95.06 | 0.0 | 21.7 | 19.5 | –1.534 |
| 11H-5, 140-150 | 101.90 | 117.09 | 0.0 | 19.3 | 16.5 | 0.2 |
| 13H-5, 140-150 | 119.40 | 138.23 | 0.0 | 19.3 | 16.8 | 1.4 |
| 15H-5, 140-150 | 139.90 | 160.53 | 0.2 | 16.7 | 14.4 | 1.4 |
| 18H-5, 140-150 | 168.10 | 188.73 | 0.3 | 15.2 | 14.0 | 2.8 |
| **172-1061A-** | | | | | | |
| 2H-4, 140-150 | 15.40 | 28.49 | 0.0 | 26.2 | 24.9 | –23.449 |
| 3H-5, 146-150 | 26.46 | 42.29 | 0.0 | 22.6 | 20.1 | –16.824 |
| 4H-5, 140-150 | 35.90 | 52.35 | 0.0 | 23.3 | 21.5 | –11.162 |
| 6H-5, 145-150 | 54.90 | 74.25 | 0.0 | 22.0 | 20.2 | –6.493 |
| 8H-5, 145-150 | 73.76 | 96.81 | 0.2 | 20.0 | 17.6 | –3.776 |
| 11H-5, 140-150 | 102.40 | 128.69 | 0.0 | 17.3 | 15.4 | –0.905 |
| 13H-5, 140-150 | 121.40 | 150.74 | 0.0 | 14.9 | 10.1 | –0.819 |
| 15H-5, 140-150 | 140.40 | 173.12 | 0.0 | 13.1 | 11.5 | 0.4 |
| 18X-4, 135-150 | 162.76 | 200.28 | 0.6 | 13.3 | 11.3 | 3.0 |
| 21X-3, 135-150 | 189.60 | 228.87 | 0.0 | 13.1 | 11.5 | 3.0 |
| 25X-1, 125-150 | 226.05 | 265.32 | 0.0 | 10.8 | 8.4 | 3.3 |
| 27X-3, 125-150 | 247.53 | 286.80 | 0.0 | 9.3 | 7.9 | 2.6 |
| 28X-4, 100-125 | 258.66 | 297.93 | 0.0 | 6.1 | 5.7 | 0.3 |
| 30X-5, 125-150 | 279.92 | 319.19 | 0.0 | 5.7 | 5.3 | 1.4 |
| 34X-1, 120-150 | 312.90 | 352.17 | 0.0 | 6.1 | 5.1 | 1.1 |
| 37X-3, 120-150 | 344.70 | 383.97 | 0.1 | 6.5 | 5.5 | –0.594 |
| **172-0161E-** | | | | | | |
| 1H-1, 145-150 | 1.45 | 1.45 | 25.2 | — | 6.2 | –14.83 |
| 1H-2, 145-150 | 2.95 | 2.95 | — | — | 9.7 | –19.167 |
| 1H-4, 145-150 | 5.35 | 5.35 | 18.2 | 12.1 | 11.2 | –21.429 |
| 1H-6, 145-150 | 8.35 | 8.35 | 12.2 | 17.6 | 14.6 | –24.003 |
| 2H-1, 145-150 | 10.85 | 10.85 | 8.2 | 21.5 | 18.1 | –26.346 |
| 2H-3, 145-150 | 13.85 | 13.85 | 5.0 | 25.2 | 21.3 | –28.059 |
| 2H-5, 132-137 | 16.72 | 16.72 | 1.1 | 26.8 | 25.4 | –30.978 |
| 2H-6, 145-150 | 18.22 | 18.22 | 0.5 | 28.2 | 25.8 | –31.293 |
| **172-1062A-** | | | | | | |
| 1H-1, 145-150 | 1.45 | 1.45 | 27.5 | 4.8 | 5.0 | –8.363 |
| 2H-1, 140-150 | 3.60 | 6.00 | 22.3 | 9.1 | 1.3 | |
| 2H-2, 140-150 | 5.10 | 7.50 | — | — | — | –15.089 |
| 2H-4, 140-150 | 8.10 | 10.50 | — | — | — | –16.099 |
| 2H-6, 140-150 | 11.10 | 13.50 | 17.2 | 13.9 | 12.3 | –17.241 |
| 3H-3, 140-150 | 16.10 | 19.02 | 14.0 | 15.6 | 15.3 | –17.279 |
| 4H-1, 140-150 | 22.60 | 27.04 | 10.5 | 17.6 | 16.6 | –17.632 |
| 4H-5, 140-150 | 28.60 | 33.04 | 8.6 | 19.2 | 19.1 | –17.936 |
| 5H-2, 140-150 | 33.60 | 38.40 | 6.8 | — | 18.9 | –18.269 |
| 6H-1, 140-150 | 41.60 | 48.62 | 4.2 | 21.2 | 17.4 | –18.972 |
| 6H-5, 140-150 | 47.60 | 54.62 | 3.5 | 19.6 | 19.2 | –19.094 |
| 7H-5, 140-150 | 57.10 | 65.14 | 1.4 | 18.8 | 16.6 | –19.729 |
| 8H-5, 140-150 | 66.60 | 74.26 | 0.5 | 18.5 | 17.4 | –20.211 |
| 9H-5, 140-150 | 76.10 | 83.10 | 0.2 | 16.2 | 16.2 | –19.452 |
| 10H-5, 140-150 | 85.60 | 92.46 | 0.3 | 14.9 | 12.8 | –19.796 |
| 12H-4, 140-150 | 103.10 | 111.00 | 0.0 | 12.6 | 10.6 | –19.373 |
| 14H-3, 135-150 | 120.55 | 128.91 | 0.0 | 8.7 | 7.2 | –15.96 |
| 16H-4, 135-150 | 140.65 | 149.67 | 0.0 | 7.6 | 6.8 | –9.863 |
| 18H-4, 135-150 | 160.05 | 171.99 | 0.3 | 8.3 | 7.7 | –4.066 |
| 20H-4, 135-150 | 179.05 | 190.99 | 0.2 | 10.6 | 7.6 | –1.326 |
| **172-1062B-** | | | | | | |
| 23X-5, 140-150 | 216.86 | 216.86 | 0.0 | 10.9 | 10.0 | 0.5 |
| 26X-5, 125-150 | 245.61 | 245.61 | 0.2 | 12.6 | 12.6 | 0.7 |
| **172-1063A-** | | | | | | |
| 1H-1, 140-150 | 1.40 | 1.40 | 25.9 | 4.5 | 5.3 | –10.46 |
| 1H-3, 140-150 | 4.40 | 4.40 | 22.3 | — | 8.8 | –14.178 |
| 2H-3, 140-150 | 8.52 | 9.38 | 14.4 | 14.8 | 15.5 | –16.427 |
| 3H-3, 140-150 | 19.20 | 20.88 | 4.5 | 24.1 | 22.4 | –21.106 |
| 3H-6, 140-150 | 23.70 | 23.70 | — | — | 23.7 | –19.654 |
| 4H-3, 140-150 | 28.70 | 30.56 | 3.6 | 22.8 | 20.4 | –22.379 |
| 4H-6, 140-150 | 33.20 | 35.06 | 2.3 | 22.3 | 20.4 | –24.611 |

## Table T1 (continued).

| Core, section, interval (cm) | Depth (mbsf) | Depth (mcd) | Sulfate (mM)* | Alkalinity (mM)* | ΣCO₂ (mM) | δ¹³C ΣCO₂ (‰ PDB) |
|---|---|---|---|---|---|---|
| 5H-3, 140-150 | 38.20 | 41.64 | 0.1 | 23.6 | 21.2 | −28.51 |
| 5H-6, 140-150 | 42.70 | 46.14 | — | 23.4 | 20.8 | −28.041 |
| 6H-3, 140-150 | 47.70 | 51.22 | 0.5 | 22.5 | 20.9 | −27.265 |
| 6H-6, 140-150 | 52.20 | 55.72 | 0.2 | 22.0 | 17.7 | −25.642 |
| 7H-3, 140-150 | 57.20 | 61.66 | 0.5 | 19.2 | 18.5 | −24.952 |
| 9H-3, 140-150 | 76.20 | 80.76 | 0.2 | 17.1 | 14.9 | −16.954 |
| 11H-5, 140-150 | 98.20 | 104.76 | 0.0 | 15.0 | 13.8 | −11.325 |
| 14H-5, 135-150 | 126.04 | 136.42 | 0.3 | 11.6 | 9.9 | −7.496 |
| 17H-5, 135-150 | 154.25 | 166.19 | 0.0 | 10.1 | 9.2 | −5.871 |
| 20H-5, 139-159 | 183.23 | 196.28 | 0.0 | 8.8 | 7.7 | −5.214 |
| 23X-4, 130-150 | 207.20 | 224.43 | 0.7 | 6.7 | 5.8 | −3.738 |
| 26X-5, 130-150 | 234.10 | 256.39 | 0.0 | 5.3 | 4.6 | −2.569 |
| 29X-3, 130-150 | 259.60 | 283.05 | 0.7 | 3.1 | 2.4 | −3.88 |
| 32X-3, 117-142 | 288.27 | 312.29 | 0.5 | 5.4 | 4.8 | −3.424 |
| 36X-5, 125-150 | 326.85 | 358.74 | 0.0 | 4.5 | 3.7 | −3.625 |
| 40X-4, 125-150 | 366.45 | 398.34 | 0.4 | 2.4 | 1.7 | −5.93 |
| 45X-5, 120-150 | 415.95 | 447.84 | 0.2 | 3.7 | 3.9 | −7.39 |

Notes: mbsf = meters below seafloor, mcd = meters corrected depth. mM = millimoles per liter or millimolar. Isotopic values in per mil (‰) relative to the Peedee belemnite (PDB) standard. * = shipboard determinations (Keigwin, Rio, Acton, et al., 1998).

**Table T2.** Carbon isotopic composition of interstitial methane and $CO_2$ gas at Leg 172 sites.

| Core, section | Depth (mbsf) | Depth (mcd) | $\delta^{13}C$ $CH_4$ (‰ PDB) | $\delta^{13}C$ $CO_2$ gas (‰ PDB) |
|---|---|---|---|---|
| 172-1054A- | | | | |
| 6H-5 | 52.51 | 54.36 | — | — |
| 10H-6 | 84.16 | 85.91 | –72.23 | — |
| 11X-3 | 89.16 | 91.21 | –72 | — |
| 13X-5 | 110.36 | 116.35 | –69.21 | — |
| 14X-5 | 119.22 | 125.21 | –68.28 | 0.9 |
| 16X-6 | 140.76 | 146.75 | –66.49 | 0.1 |
| 18X-2 | 154.06 | 160.05 | –67.83 | 2.3 |
| 20X-2 | 173.36 | 179.35 | –67.41 | 3.8 |
| 22X-5 | 197.16 | 203.15 | –65.75 | 2.0 |
| 172-1055B- | | | | |
| 8H-1 | 61.50 | 69.31 | –79.95 | — |
| 9H-1 | 71.00 | 79.51 | –78.5 | — |
| 11H-2 | 90.00 | 102.07 | –77.83 | –3.42 |
| 13H-3 | 109.00 | 124.60 | –72.54 | — |
| 172-1058A- | | | | |
| 8H-1 | 67.60 | 74.29 | –80.15 | — |
| 9H-1 | 76.43 | 84.10 | –79.03 | — |
| 11H-2 | 97.00 | 106.78 | –76.02 | — |
| 12H-3 | 107.58 | 119.67 | –74.78 | — |
| 13H-3 | 117.56 | 130.93 | –73.46 | — |
| 15H-3 | 136.15 | 152.42 | –72.68 | — |
| 172-1059A- | | | | |
| 2H-5* | 11.25 | 13.32 | –100.6 | –30.53 |
| 2H-6* | 12.75 | 14.82 | –98.2 | –26.19 |
| 3H-1* | 14.75 | 17.30 | –97.14 | –22.64 |
| 3H-2* | 16.25 | 18.80 | –96.16 | –19.17 |
| 3H-3* | 17.75 | 20.30 | –95.27 | –21.66 |
| 3H-4* | 19.25 | 21.80 | –93.62 | –20.54 |
| 6H-1 | 42.47 | 52.47 | –85.76 | — |
| 172-1060A- | | | | |
| 8H-2 | 67.57 | 79.64 | –84.99 | — |
| 11H-1 | 95.98 | 111.17 | –77.38 | — |
| 14H-3 | 126.82 | 147.45 | –80.58 | — |
| 16H-5 | 145.58 | 169.44 | –79.11 | — |
| 18H-4 | 166.65 | 187.28 | –77.68 | — |
| 172-1061A- | | | | |
| 6H-1 | 48.91 | 68.26 | –88.3 | –4.4 |
| 9H-1 | 77.03 | 102.08 | –85.56 | — |
| 13H-3 | 117.15 | 146.49 | –83.62 | — |
| 16H-5 | 147.44 | 182.56 | –79.22 | — |
| 20X-4 | 182.07 | 221.34 | –76.97 | — |
| 24X-4 | 220.91 | 260.18 | –76.15 | — |
| 30X-4 | 277.67 | 316.94 | –75.52 | — |
| 34X-2 | 313.68 | 352.95 | –74.2 | — |
| 37X-1 | 341.07 | 380.34 | –73.56 | — |
| 172-1062A- | | | | |
| 16H-1 | 136.28 | 145.30 | –85.08 | — |
| 18H-3 | 157.27 | 169.21 | –83.18 | — |
| 21X-4 | 187.08 | 196.04 | –79.42 | — |
| 172-1063A- | | | | |
| 12H-1 | 100.66 | 107.66 | –91.38 | — |
| 16H-1 | 139.25 | 150.53 | –87.36 | — |
| 20H-1 | 177.48 | 190.53 | –84.81 | — |
| 24X-2 | 209.69 | 228.92 | –82.07 | — |
| 28X-3 | 250.18 | 273.63 | –82.52 | — |
| 32X-2 | 291.46 | 315.48 | –82.02 | — |
| 34X-6 | 312.11 | 339.28 | –79.53 | — |
| 38X-1 | 341.92 | 373.81 | –81.6 | — |
| 45X-6 | 416.32 | 448.21 | –82.81 | — |

Notes: mbsf = meters below seafloor, mcd = meters corrected depth. Isotopic values in per mil (‰) relative to the Peedee belemnite (PDB) standard. * = Reeburgh squeezer samples.